Published in final edited form as:
J Immunol. 2015 January 1; 194(1): 307–315. doi:10.4049/jimmunol.1401999.

Altered lymph node composition in diphtheria toxin receptor-based mouse models to ablate dendritic cells

Janneke van Blijswijk[*], **Barbara U. Schraml**[*,†], **Neil C. Rogers**[*], **Paul G. Whitney**[*,‡], **Santiago Zelenay**[*], **Sophie E. Acton**[*], and **Caetano Reis e Sousa**[*,1]

[*]Immunobiology Laboratory, Cancer Research UK, London Research Institute, Lincoln's Inn Fields Laboratories, 44 Lincoln's Inn Fields, London WC2A 3LY, United Kingdom

Abstract

Dendritic cells (DCs) are key regulators of innate and adaptive immunity. Our understanding of immune function has benefited greatly from mouse models allowing for selective ablation of DCs. Many such models rely on transgenic diphtheria toxin receptor (DTR) expression driven by DC-restricted promoters. This renders DCs sensitive to DT but is otherwise thought to have no effect on immune physiology. Here, we report that, unexpectedly, mice in which DTR is expressed on conventional DCs display marked lymph node (LN) hypocellularity and reduced frequency of DCs in the same organs but not in spleen or non-lymphoid tissues. Intriguingly, in mixed bone marrow (BM) chimeras the phenotype conferred by DTR-expressing DCs is dominant over control BM-derived cells, leading to small LNs and an overall paucity of DCs independently of the genetic ability to express DTR. The finding of alterations in LN composition and size independently of diphtheria toxin challenge suggests that caution must be exercised when interpreting results of experiments obtained with mouse models to inducibly deplete DCs. It further indicates that DTR, a member of the epidermal growth factor family, is biologically active in mice. Its use in cell ablation experiments needs to be considered in light of this activity.

Keywords

dendritic cells; Langerhans cells; diphtheria toxin; diphtheria toxin receptor; neutrophilia; cell depletion

Address correspondence to: Dr. Caetano Reis e Sousa, Immunobiology Laboratory, Cancer Research UK, London Research Institute, Lincoln's Inn Fields Laboratories, 44 Lincoln's Inn Fields, London WC2A 3LY, Tel: + 44 20 7269 2832, FAX: +44 20 7269 2833, caetano@cancer.org.uk.

[1]C.R.S. is funded by Cancer Research UK, a prize from Fondation Bettencourt-Schueller, and a grant from the European Research Council (ERC Advanced Researcher Grant AdG-2010-268670). J.v.B. was supported by Boehringer Ingelheim Fonds, B.U.S. was supported by an EMBO long-term fellowship, P.G.W. was supported by an Overseas Biomedical Fellowship from the NHMRC of Australia (APP1013641), and S.E.A. was supported by a Henry Wellcome Fellowship (WT089009MA).

[†]Current address: Institute for Medical Microbiology, Immunology and Hygiene, Technische Universität München, Munich 81675, Germany

[‡]Current address: Peter Doherty Institute for Infection and Immunity, The University of Melbourne, Parkville, Victoria 3000, Australia

Conflict of interest: The authors declare no competing financial interests.

Introduction

Dendritic cells (DCs) are key inducers of adaptive immunity and tolerance, as well as regulators of innate immunity. The DC family comprises several subsets that are defined based on function, surface marker expression, localization in the body and ontogeny (1-5). It is common to sub-divide DCs into plasmacytoid DCs (pDCs) and conventional DCs (cDCs) (1-5). A further sub-classification of cDCs is made within lymph nodes (LNs) to distinguish between resident DCs (resDCs) and migratory DCs (migDCs). While the former derive from precursors that enter LNs via the blood, migDCs derive from DCs in non-lymphoid tissues that immigrated into draining LNs via afferent lymphatics (1-4). ResDCs and migDCs are heterogeneous and comprise multiple cDC subsets, often referred to as the $CD8\alpha^+$ cDC and the $CD11b^+$ cDC families.

Mouse models to deplete DCs have proven useful tools to elucidate DC function *in vivo*. The first such model exploited CD11c expression to drive expression of simian diphtheria toxin receptor (DTR) fused to GFP in DCs (6). DTR is also called heparin-binding EGF-like growth factor (HB-EGF) and is a membrane-anchored protein (7). The EGF portion can be cleaved by metalloproteinases, releasing a soluble EGF-like ligand. As simian and human HB-EGF bind diphtheria toxin (DT) with about 10^5 times higher affinity than rodent versions, expression of primate DTR in murine cells by transgenesis renders the latter highly susceptible to DT intoxication, resulting in block of protein translation and cell death (8). CD11c is commonly used as marker for DCs and, in CD11c-DTR mice, DTR expression is driven by a minimal CD11c promoter (6). This allows for DTR expression in cDCs, pDCs and Langerhans cells (LC) and makes the cells sensitive to ablation by DT. However, CD11c-DTR mice die after repeated DT injections, probably because of aberrant DTR expression on non-immune cells, such as epithelial cells of the gut (9). Therefore, long-term DC depletion can only be achieved in radiation chimeras in which wild-type mice are reconstituted with CD11c-DTR bone marrow (BM). Furthermore, CD11c is also expressed by some macrophages, plasmablasts, Ly-$6C^{low}$ monocytes, activated T cells and NK cells, resulting in DTR expression and DT-mediated depletion of these cell types (6, 10, 11). More recently, improved models have been developed in which DTR is more highly restricted to DCs (CD11c-DOG and zDC-DTR mice) (10, 12) or is expressed selectively in specific DC subsets (Langerin-DTR, BDCA2-DTR, SiglecH-DTR, CD205-DTR and Clec9a-DTR mice) (13-18). All these models allow for successful DT-mediated ablation of the target DC populations and have been instrumental in advancing DC research even if they suffer from limitations, predominantly due to mis-expression of DTR or side effects such as neutrophilia following DT-mediated DC ablation (19-21). Nevertheless, no immune abnormalities have been reported in any models expressing DTR on DCs in the absence of DT treatment, despite the fact that DTR, being an EGF family member, might potentially be able to engage murine EGF receptors.

We have recently shown that DNGR-1 (also known as CLEC9A) is specifically expressed on conventional DC precursors and pre-DCs (5). As a consequence, mice expressing Cre recombinase under the control of the *Clec9a* locus can be used to fate map those precursors *in vivo* when crossed to a ROSA26-LSL-YFP reporter line (5). ROSA26 is a locus that is often targeted to drive constitutive and ubiquitous gene expression in mice (22). In

ROSA26-LSL (lox-stop-lox) strains, expression is prevented by a STOP cassette flanked by loxP sites that can be irreversibly excised through the action of Cre recombinase. We therefore predicted that the same Clec9a-Cre mice could be used to generate DT-sensitive DCs *in vivo* if crossed to a ROSA26-LSL-DTR strain (23). Here, we report that such mice indeed allow for specific DT-dependent DC ablation. However, they display LN hypocellularity and reduced frequencies of DCs in LNs even in the absence of DT injection. Moreover, the LN phenotype induced by DTR-expressing DCs is dominant over that of DCs lacking the receptor. Finally, we report that the LN hypocellularity and reduced frequencies of DCs in LNs is a common feature of other mouse models in which DTR is expressed on DCs. Thus, transgenic expression of human or simian HB-EGF in mice is not without consequences and caution and the use of proper controls is warranted when using and reporting on any mouse model in which DTR is expressed on DCs and, perhaps, other cells.

Materials and Methods

Mice

Clec9a-Cre (5), ROSA26-LSL-iDTR (23), CD11c-Cre (24), CD11c-DTR (6), Langerin-DTR (14), CD11c-DOG (10), CD19-Cre (25), DEREG (26), C57BL/6J and B6.SJL mice were bred at Cancer Research UK in specific pathogen-free conditions. Eight to sixteen week old mice were used in all experiments, unless otherwise indicated. Littermates or ROSA26-LSL-iDTR mice were used as controls. All animal experiments were performed in accordance with national and institutional guidelines for animal care and were approved by the London Research Institute Animal Ethics Committee and by the UK Home Office.

To deplete DCs in Clec9a$^{+/Cre}$ROSA^{iDTR} mice, mice were injected i.p. with 12ng/g body weight diphtheria toxin (Sigma D0564) and analyzed 24 hours later.

Radiation chimeras

CD45.2^{+} C57BL/6J mice were irradiated twice with 6.6 Gray, separated by 4 hours. Mice were injected i.v. 24 hours later with 2×10^{6} total BM cells at a 1:1 mixture of CD45.1^{+} B6.SJL and CD45.2^{+} Clec9a$^{+/+}$ROSA^{iDTR} or Clec9a$^{+/Cre}$ROSA^{iDTR} BM. Mice were analyzed 3-6 months after reconstitution.

Cell isolation

Inguinal LNs were used for analysis of sdLNs. Spleens, thymus, LNs and Peyer's patches were digested with Collagenase IV (200U/ml; Worthington) and DNase I (0.2mg/ml, Roche). For spleens, red blood cells were lysed with Red Blood Cell Lysis Buffer (Sigma).

Isolation of DC from small intestines (SIs) was adapted from reference (27). SIs were sliced open after removal of Peyer's patches, rinsed and cut into small pieces. Epithelial cells and intraepithelial lymphocytes were removed by incubating SI pieces in RMPI containing 25mM HEPES, L-glutamine, Penicillin/Streptomycin, 50μM β-mercaptoethanol, 5mM EDTA (all Gibco), 3% fetal calf serum and 0.145mg/ml DL-dithiothreitol (Sigma) for 20 min at 37 °C while shaking. The suspension was strained through a sieve and SI pieces were collected in RMPI containing 25mM HEPES, L-glutamine, Penicillin/Streptomycin, 50μM

β-mercaptoethanol and 2mM EDTA (all Gibco), vortexed and strained again. This last step was repeated twice. SIs were digested with Collagenase IV (200U/ml) and DNase I (0.2mg/ml) in 10 ml RPMI medium for one hour at 37 °C.

For the analysis of dermis and epidermis both ears were collected and split into dorsal and ventral halves. Split ears were incubated for 1 hour at 37°C, while floating dermis-down on 2U/ml Dispase II (Roche) in PBS. Epidermis and dermis were separated and digested separately with Collagenase IV (200U/ml; Worthington) and DNase I (0.2mg/ml, Roche) in RPMI for 1 hour at 37°C.

For analysis of SIs, dermis and epidermis, leukocytes were enriched by Percoll gradient centrifugation (GE Healthcare).

Flow Cytometry

Samples were collected on a LSR Fortessa flow cytometer (BD Biosciences) and analyzed using FlowJo software (TreeStar Inc.). Gating strategies are shown in figure S1.

The following antibodies were purchased from BD Bioscience: CD8α-FITC (53-6.8), Ly6c-FITC (AL-21), CD45.1-FITC (A20), CD45.2-FITC (104), CD3-FITC, CD3-PE (145-2C11), CD16/32 (2.4G2; Fc block), CD11c-FITC (HL3), B220-FITC and B220-PE (RA3-6B2).

The following antibodies were purchased from Biolegend: CD11c-PerCP/Cy5.5 (N418), CD64-PE (X5-4/7.1), Gr-1-FITC, (RB-8C5), CD103-PerCP/Cy5.5 (2E7), CD326-AF647 (Ep-CAM, G8.8) and CD45.2-PeCy7 (104).

The following antibodies were purchased from eBioscience: CD45.1-PerCP/Cy5.5, CD45.1-PeCy7 (A20), MHCII I-A/I-E-AF700, MHCII I-A/I-E-APC-eFluor780 (M5/114.15.2), CD8α -eFluor605nc (53-6.8), CD11b-AF700, CD11b-APC-eFluor-780, CD11b-eFluor605nc (M1/70), Ly6G-AF700 (RB6-8C5), CD103-PE and CD103-APC (2E7).

CD207-AF488 (929F3.01) was purchased from Dendritics. Biotinylated polyclonal anti-DTR (hHB-EGF) was purchased from R&D systems and detected with streptavidin-PE (BD biosciences).

Dapi was used to exclude dead cells, except for when cells were stained intracellularly with anti-CD207-AF488, when dead cells were excluded by live/dead fixable violet dye (Invitrogen). For intracellular staining, cells were stained for surface markers followed fixation and intracellular staining with FIX&PERM (ADG) according to the manufacturer's protocol.

Microscopy

Frozen sections from inguinal LNs were air dried, fixed for 10min in 2% PFA and washed in PBS. Blocking was performed for 30min at room temperature in 10% goat serum (Sigma) in PBS. Sections were stained for 1 hour at room temperature with B220-APC (RA3-6B2, BD Bioscience) and CD3-FITC (145-2C11, BD Bioscience) in blocking buffer. Images were acquired on a LSM710 upright confocal microscope (Zeiss) using a 10x objective and analyzed with Bitplane Imaris software.

Statistical analysis

Results are depicted as mean ± SD. Unpaired student's t tests were performed to calculate p-values.

Results

Efficient depletion of DCs in Clec9a$^{+/Cre}$ROSA^{iDTR} mice upon DT injection

We crossed Clec9a-Cre "knock-in" mice to a ROSA26-LSL-iDTR strain (23) to generate Clec9a$^{+/Cre}$ROSA^{iDTR} mice. All mice used for experiments were heterozygous for Cre recombinase and, therefore, DNGR-1 sufficient. We did not observe any differences between mice harboring either one or two copies of DTR and therefore combined them in our experiments. On average 93±1% of CD8α^{+} DCs and 59±5% of CD11b^{+} DCs, but no other cell types, expressed DTR in the spleens of Clec9a$^{+/Cre}$ROSA^{iDTR} animals (figure 1A and data not shown). The fact that circa 40% of CD11b^{+} splenic DCs were negative for DTR expression is in line with the previously observed incomplete penetrance of Cre activity in heterozygous Clec9a-Cre mice (5).

When Clec9a$^{+/Cre}$ROSA^{iDTR} mice were injected with DT, virtually all splenic CD8α^{+} DCs and most CD11b^{+} DCs were depleted 24 hours post-treatment (figure 1B,C) while other immune cell populations were spared (data not shown). Notably, DT-mediated DC depletion in this strain was not accompanied by neutrophilia and monocytosis (figure 1D), at least at this time point, in contrast to depletion in other models such as CD11c-DOG mice and CD11c-DTR mice (12, 20, 21). Therefore, Clec9a$^{+/Cre}$ROSA^{iDTR} mice can be used to successfully and specifically deplete DCs using DT with minimal side effects caused by DT treatment.

LNs of Clec9a$^{+/Cre}$ROSA^{iDTR} mice show hypocellularity and reduced frequency of DCs

As expected, DTR was also expressed by DCs in skin-draining LNs (sdLNs) of Clec9a$^{+/Cre}$ROSA^{iDTR} mice (figure S2A) and allowed for their depletion upon DT injection (Figure S2B). However, when analyzing sdLNs, we noticed that both resDCs and migDCs were present at reduced frequency in PBS-treated Clec9a$^{+/Cre}$ROSA^{iDTR} mice compared to PBS-treated genetic control mice (figure S2B). To follow-up on this unexpected observation, we analyzed in greater detail the spleens, thymi and LNs of untreated Clec9a$^{+/Cre}$ROSA^{iDTR} mice. We confirmed that untreated Clec9a$^{+/Cre}$ROSA^{iDTR} mice display a marked reduction in frequency of both resDCs and migDCs in sdLNs when compared to Cre-negative controls (figure 2AB). A similar decrease in frequency of DCs was observed in mesenteric LNs (mesLNs; figure 2B). In contrast, DC frequency in the spleen and thymus was identical between Clec9a$^{+/Cre}$ROSA^{iDTR} mice and Cre-negative controls (figure 2B). DC frequency was also identical in epidermis, dermis, small intestine and Peyer's patches of Clec9a$^{+/Cre}$ROSA^{iDTR} mice when compared to Cre-negative controls (figure 2C). Together, these observations suggest that only lymphoid organs with an afferent lymph supply and, consequently, possessing migDCs are affected.

In addition to lower DC frequency, we also observed a marked reduction in the cellularity of sdLNs and mesLNs (figure 2D) in untreated Clec9a$^{+/Cre}$ROSA^{iDTR} mice when compared to

Europe PMC Funders Author Manuscripts

their genetic controls. This accentuated the dearth of LN DCs and was not seen in the spleen and thymus, which displayed normal cellularity (figure 2D). All immune cell populations were reduced in number in the LNs of Clec9a$^{+/Cre}$ROSA^{iDTR} mice, contributing to the overall hypocellularity, although the loss of T cells was most acute, leading to an increase in the ratio of B to T cells (figure 2E and data not shown). However, despite hypocellularity and increased B/T cell ratio, the overall LN architecture appeared intact (figure 2F).

To determine the influence of age on the observed phenotype, we assessed DC frequency and cellularity in spleen and sdLNs of one year old Clec9a$^{+/Cre}$ROSA^{iDTR} mice and Cre-negative controls. In line with our previous findings, there was no difference in splenic DC frequency or spleen cellularity between Clec9a$^{+/Cre}$ROSA^{iDTR} and Cre-negative control mice (figure S3AB). However, we again observed a reduced frequency of migDCs in sdLN of old Clec9a$^{+/Cre}$ROSA^{iDTR} mice compared to control mice (figure S3AB). Furthermore, cellularity was reduced in sdLN of old Clec9a$^{+/Cre}$ROSA^{iDTR} mice (figure S3AB). In this experiment we did not observe a difference in resDC frequency in sdLNs.

In sum, the cellularity and composition of LNs but not spleen or thymus is markedly altered in Clec9a$^{+/Cre}$ROSA^{iDTR} mice and the phenotype appears to be maintained with ageing. These results were unexpected, as DTR transgene expression in DCs is widely used in mouse models of inducible DC depletion without reports of adverse effects in the absence of DT treatment.

The phenotype of Clec9a$^{+/Cre}$ROSA^{iDTR} bone marrow is dominant over WT bone marrow in mixed bone marrow chimeras

DTR expression could be toxic to DCs, acting in a cell-autonomous fashion to decrease survival or migration. Alternatively, expression of DTR on DCs might act in a non-cell-autonomous manner to broadly influence the LN environment and all DCs within it. To distinguish these possibilities, we generated mixed BM chimeras with a 1:1 mixture of CD45.1^{+} wild-type (WT) BM and CD45.2^{+} Clec9a$^{+/+}$ROSA^{iDTR} (Cre-negative) or Clec9a$^{+/Cre}$ROSA^{iDTR} (Cre-positive) BM. Full chimerism was confirmed by measuring the ratio of CD45.1 to CD45.2 in blood neutrophils (data not shown). We first compared frequencies of resDCs and migDCs within the total CD45.1^{+} or CD45.2^{+} population in both sdLNs and mesLNs. Among CD45.2^{+} cells, both resDC and migDC frequencies were reduced in mice receiving Cre-positive BM compared to animals receiving control Cre-negative BM (figure 3A). These data indicated that the paucity of DCs in Clec9a$^{+/Cre}$ROSA^{iDTR} mice could not be rescued by the presence of WT cells. Moreover, we were surprised to find that the frequencies of both resDCs and migDCs in the CD45.1^{+} WT compartment were similarly reduced in chimeras receiving Cre-positive BM but not in chimeras receiving Cre-negative control BM (figure 3A). Therefore, DTR does not appear to merely affect in a cell autonomous manner those DCs that express it. Rather, Clec9a$^{+/Cre}$ROSA^{iDTR} BM-derived cells have a dominant effect that reduces the frequency of DCs deriving from WT BM. This dominance was also reflected in the size of sdLNs and mesLNs, but not spleen, which was reduced in chimeras receiving Cre-positive BM when compared to size in control chimeras (figure 3B and data not shown). In summary, the

hypocellularity and relative reduction of DCs in LNs of Clec9a$^{+/Cre}$ROSA^{iDTR} mice are replicated in mixed chimeras containing Clec9a$^{+/Cre}$ROSA^{iDTR} BM.

Reduced DC frequencies and LN hypocellularity in other mice where DTR is expressed on DCs

The LN hypocellularity and reduced frequencies of DC subsets in LNs could be the result of targeting the Clec9a locus, targeting the ROSA26-locus, or expressing DTR on DCs. Arguing against the first two possibilities, our original reporter mice in which the Clec9a-Cre strain was crossed to ROSA26-LSL-YFP mice all had normal size LNs and unaltered LN composition (figure S4A). Nevertheless, to determine whether the phenotype was exclusive to the use of the Clec9a-Cre strain, we crossed CD11c-Cre mice (24) to ROSA26-LSL-iDTR mice. CD11c-Cre^{+ve}ROSA^{iDTR} mice also showed hypocellularity of sdLNs and mesLNs, but not spleen, and reduced frequencies of migDCs in sdLNs and mesLNs (figure 4A, S4B and data not shown). ResDC frequency was also reduced in mesLNs of CD11c-Cre^{+ve}ROSA^{iDTR} mice (figure S4B) and there was a trend for reduced frequencies of resDCs in sdLNs, although this did not reach statistical significance (figure 4A). Thus, CD11c-Cre^{+ve}ROSA^{iDTR} mice largely phenocopy Clec9a$^{+/Cre}$ROSA^{iDTR} mice.

Next, we analyzed the original CD11c-DTR mice (6), which have been widely used to study DC functions *in vivo*. Similar to Clec9a$^{+/Cre}$ROSA^{iDTR} mice, CD11c-DTR mice showed reduced frequencies of resDCs and migDCs in sdLNs and mesLNs and hypocellularity of the same organs (figure 4B and S4C). As CD11c-DTR mice do not express DTR from the ROSA26-locus, this finding excludes the possibility that the ROSA26-LSL-iDTR strain is responsible for the observed phenotype. Together, these results indicate that paucity of LN DCs and hypocellularity of LNs is a feature common to Clec9a$^{+/Cre}$ROSA^{iDTR}, CD11c-Cre^{+ve}ROSA^{iDTR} and CD11c-DTR mice.

The above strains all allow for expression of DTR on multiple DC subtypes. To test if expression of DTR on a subset of DCs is sufficient to induce the observed phenotype, we used Langerin-DTR mice (14). In Langerin-DTR mice, DTR is under control of the CD207 locus, which is active in LCs, CD103^{+} dermal DCs and some CD8α^{+} resDCs. As observed for the other mouse strains, Langerin-DTR mice displayed reduced frequencies of migDCs in sdLNs and hypocellularity of the same organ (figure 4C). This phenotype was not observed in mesLNs, unlike in the other strains tested (figure S4D). Further investigation revealed that the difference between sdLNs and mesLNs in Langerin-DTR mice correlated with levels of DTR expression: very little DTR expression was observed on DCs from mesLNs while DTR was expressed on both resDCs and migDCs subsets in sdLNs (figure 4D and S4E). In sum, analysis of Langerin-DTR mice suggests that DTR expression on a subset of DCs is sufficient to induce reduced migDCs accumulation in LNs and LN hypocellularity. Moreover, the effect of DTR appears local and not systemic as in Langerin-DTR mice the affected LNs are those in which higher DTR expression is found on DCs.

We also tested CD11c-DOG mice, which express DTR on DCs1. Like CD11c-DTR mice, these mice also exploit CD11c expression to express DTR on DCs. However, CD11c-DOG mice utilize the CD11c locus control region instead of a minimal promoter to drive DTR expression (6, 10). Surprisingly, we found no difference in sdLN and mesLN cellularity and

Europe PMC Funders Author Manuscripts

DC frequencies in sdLNs and mesLNs between CD11c-DOG mice and controls (figure 4E and S4F). However, we noticed that resDCs in sdLNs and mesLNs of CD11c-DOG mice expressed DTR at very low levels (figure 4F and S4G). Moreover, DTR expression on migDCs in sdLNs and mesLNs of CD11c-DOG mice was undetectable by staining (figure 4F and S4G). These results suggest that low DTR expression on resDCs alone may not be not sufficient to confer the LN phenotype.

Finally, to address whether DTR expression on other immune cells leads to a similar LN phenotype, we crossed CD19-Cre mice (25) to ROSA26-LSL-iDTR mice, to drive expression of DTR on B cells. Notably, frequencies of B cells and resDCs were not decreased in sdLNs and mesLNs of $CD19^{+/Cre}ROSA^{iDTR}$ mice (figure 5A). MigDC frequencies were unaltered in sdLNs, but slightly decreased in mesLNs (figure 5A), although this decrease was much smaller than that observed in the DC-restricted DTR models tested here. $CD8\alpha^{+}$ DCs in the spleen of $CD19^{+/Cre}ROSA^{iDTR}$ mice were unaltered, while $CD11b^{+}$ DC frequency was increased in $CD19^{+/Cre}ROSA^{iDTR}$ mice (figure 5A). Furthermore, $CD19^{+/Cre}ROSA^{iDTR}$ mice displayed only a mild reduction in cellularity of sdLNs, but not of the mesLNs or spleen (figure 5A). We also analyzed DEREG mice in which DTR is expressed on regulatory T cells (Tregs) (26). DEREG mice displayed a mild decrease in the frequency of migDCs in both sdLNs and mesLNs compared to controls, while resDCs and DCs in the spleen were unaltered (figure 5B). However, in contrast to mice expressing DTR on DCs, DEREG mice did not show signs of LN hypocellularity (figure 5B). In summary, neither $CD19^{+/Cre}ROSA^{iDTR}$ mice nor DEREG mice fully recapitulate the phenotype of dramatic hypocellularity of LNs and reduced frequencies of resDCs and migDCs in LNs. However, LNs of $CD19^{+/Cre}ROSA^{iDTR}$ and DEREG mice are not identical to those in the respective controls perhaps because of DTR expression on B cells or Tregs or an unknown cause (e.g., haploinsufficiency of CD19 or aberrations due to BAC integration). Overall, these results suggest that expression of DTR on a large fraction of LN cells is not necessarily detrimental but that its expression specifically on DCs has unexpected consequences.

Discussion

Mouse models to deplete DCs are useful tools to elucidate immune function. Many of these models rely on transgenic DTR expression driven by promoters more or less restricted to DC. Despite the fact that the first such model, the CD11c-DTR mouse (6), was generated over ten years ago and has since been used extensively (19), mice in which simian or human DTR is forcibly expressed on DCs have not been reported to display immune abnormalities. Here, we describe the unexpected finding that they display reduced LN cellularity and a profound decrease in the relative frequency of DCs in LNs in the absence of DT treatment.

We tested five different mouse models in which DTR is forcibly expressed in DCs ($Clec9a^{+/Cre}ROSA^{iDTR}$, $CD11c\text{-}Cre^{+ve}ROSA^{iDTR}$, CD11c-DTR, Langerin-DTR and CD11c-DOG mice). Although this list includes widely-used models for DC depletion, it is not exhaustive. In particular, we have not tested the recently described zDC-DTR mice (12). Furthermore, the data presented here do not allow us to assess whether it is necessary and/or sufficient for DTR to be expressed by a particular subset of DCs to confer the LN

phenotype. In this regard, Clec9a-DTR mice (18), SiglecH-DTR and BDCA2-DTR mice (15, 16) may be used to address the consequences of expressing DTR on CD8α-like cDCs or pDCs, although there are at present no mouse models that allow DTR expression exclusively by $CD11b^+$ cDCs. In addition, it will be interesting to assess LN cellularity and phagocyte frequency in mice in which DTR is forcibly expressed on monocytes or macrophages.

We do not at present understand the mechanistic basis for our findings, although the data presented here may provide some clues. As DC frequencies were unaltered in the spleen and non-lymphoid tissues in the mouse models examined here, and because in Langerin-DTR mice the sdLNs, but not mesLNs were affected, which correlated with DTR expression, a defect at the level of DC precursors or their ability to seed tissues is unlikely. Rather, only tissues with an afferent lymph supply seem to be affected and the paucity of migDCs in LNs likely reflects an impairment in their migration from peripheral sites, or a reduced lifespan once in the LN. Reduced lifespan might also explain the decrease in LN resDCs frequencies. Furthermore, the alteration in LN composition and function is not imprinted during mouse development as it can be conferred to adult mice by transplantation of BM from affected mice and, remarkably, acts dominantly over WT BM. We therefore speculate that DCs expressing DTR modulate the LN microenvironment, either via a soluble factor or cell-cell contact, to make it unfavorable for DC immigration. This factor could be DTR itself, either shed from, or expressed on the DC surface, or another factor made by DCs or other cells, upon engagement of DTR on DCs and EGF receptors on adjacent cells. Within the LN, either the lack of DCs or, again, a modulation of the microenvironment by DTR-expressing DCs, may impair the homing to, or retention in the LN of lymphocytes, especially T cells, resulting in LN hypocellularity. In this regard, it is notable that paucity of DCs has been shown to cause shutdown of high endothelial venules (HEVs) (28). Furthermore, when DC migration to LNs is impaired due to a lack of CCR7, LNs also show a reduced number of HEVs, reduced LN size and T cell lymphopenia in LNs (29). Given these hypotheses, we have tested whether DTR-expressing DCs display an alteration in their migratory ability, looked for alterations in HEV phenotype and searched for an effect of DTR-expressing DCs on LN stroma leading to reduced production of lymphocyte chemoattractants (data not shown). Our conclusions to-date are that none of these scenarios can fully explain the phenotype observed (data not shown). We cannot exclude that the phenotype observed is a consequence of a complex interaction with the external environment. In this regard, it will be of interest to analyze the same strains across multiple animal facilities or after rederivation into a gnotobiotic environment.

Whatever the underlying mechanism, our findings indicate a need for caution when interpreting results obtained with DTR-based mouse models to inducibly deplete DCs, as the steady-state immune system in such mice clearly differs from that of controls. In this regard, it is important to note that small LN size has recently been shown to markedly impact immune responses and resistance to infection (30). Why the phenotype described here appears to have passed unnoticed or at least unreported is unclear but may in part be due to the tendency to use PBS-injected DTR-expressing mice (rather than littermates not encoding DTR) as controls for mice receiving DT. Based on our findings, we would suggest that both types of controls are warranted and that some of the changes in immune responses observed upon DT-mediated DC depletion might in fact be a composite caused by acute loss of DCs

Europe PMC Funders Author Manuscripts

superimposed on underlying LN defects. Our findings also suggest that simian HB-EGF possesses biological activities in mice that cannot be ignored. As such, DTR expression on other cell types, including those outside the immune system, might alter their cell biology or, as shown here, that of their immediate environment. The latter may require shedding via the action of cell-specific metalloproteinases, explaining why expression on some cells (e.g., B cells or Tregs) is apparently innocuous while that is not the case for expression on DCs. Clearly, the use of DTR in mice has pitfalls that might impact on experimental approaches and need to be tempered with the great advantages awarded by the ability to ablate cells at will.

Supplementary Material

Refer to Web version on PubMed Central for supplementary material.

Acknowledgements

We are grateful to Giovanna Lombardi and Clare Bennett for providing mouse strains. We thank the FACS Laboratory of the London Research Institute for technical support and the Biological Resources staff for animal care and assistance with mouse experiments.

Abbreviations

BM	bone marrow
Clec9a	C-type lectin domain family 9, member A
DC	dendritic cell
DNGR-1	Dendritic cell NK lectin group receptor-1
DT	diphtheria toxin
DTR	DT receptor
LC	Langerhans cell
LN	lymph node
mesLN	mesenteric LN
migDC	migratory DC
pDC	plasmacytoid DC
resDC	resident DC
sdLN	skin-draining LN
WT	wild-type

References

1. Geissmann F, Manz MG, Jung S, Sieweke MH, Merad M, Ley K. Development of monocytes, macrophages, and dendritic cells. Science. 2010; 327:656–661. [PubMed: 20133564]
2. Hashimoto D, Miller J, Merad M. Dendritic Cell and Macrophage Heterogeneity In Vivo. Immunity. 2011; 35:323–335. [PubMed: 21943488]

3. Heath WR, Carbone FR. Dendritic cell subsets in primary and secondary T cell responses at body surfaces. Nat Immunol. 2009; 10:1237–1244. [PubMed: 19915624]
4. Steinman RM, Idoyaga J. Features of the dendritic cell lineage. Immunol Rev. 2010; 234:5–17. [PubMed: 20193008]
5. Schraml BU, van Blijswijk J, Zelenay S, Whitney PG, Filby A, Acton SE, Rogers NC, Moncaut N, Carvajal JJ, Reis e Sousa C. Genetic tracing via DNGR-1 expression history defines dendritic cells as a hematopoietic lineage. Cell. 2013; 154:843–858. [PubMed: 23953115]
6. Jung S, Unutmaz D, Wong P, Sano G-I, De los Santos K, Sparwasser T, Wu S, Vuthoori S, Ko K, Zavala F, Pamer EG, Littman DR, Lang RA. In Vivo Depletion of CD11c+ Dendritic Cells Abrogates Priming of CD8+ T Cells by Exogenous Cell-Associated Antigens. Immunity. 2002; 17:211–220. [PubMed: 12196292]
7. Higashiyama S, Iwabuki H, Morimoto C, Hieda M, Inoue H, Matsushita N. Membrane-anchored growth factors, the epidermal growth factor family: Beyond receptor ligands. Cancer Science. 2008; 99:214–220. [PubMed: 18271917]
8. Saito M, Iwawaki T, Taya C, Yonekawa H, Noda M, Inui Y, Mekada E, Kimata Y, Tsuru A, Kohno K. Diphtheria toxin receptor-mediated conditional and targeted cell ablation in transgenic mice. Nat Biotechnol. 2001; 19:746–750. [PubMed: 11479567]
9. Zaft T, Sapoznikov A, Krauthgamer R, Littman DR, Jung S. CD11chigh dendritic cell ablation impairs lymphopenia-driven proliferation of naive and memory CD8+ T cells. J Immunol. 2005; 175:6428–6435. [PubMed: 16272295]
10. Hochweller K, Striegler J, Hämmerling GJ, Garbi N. A novel CD11c.DTR transgenic mouse for depletion of dendritic cells reveals their requirement for homeostatic proliferation of natural killer cells. European journal of immunology. 2008; 38:2776–2783. [PubMed: 18825750]
11. Probst HC, Tschannen K, Odermatt B, Schwendener R, Zinkernagel RM, Van Den Broek M. Histological analysis of CD11c-DTR/GFP mice after in vivo depletion of dendritic cells. Clin. Exp. Immunol. 2005; 141:398–404. [PubMed: 16045728]
12. Meredith MM, Liu K, Darrasse-Jeze G, Kamphorst AO, Schreiber HA, Guermonprez P, Idoyaga J, Cheong C, Yao KH, Niec RE, Nussenzweig MC. Expression of the zinc finger transcription factor zDC (Zbtb46, Btbd4) defines the classical dendritic cell lineage. J Exp Med. 2012
13. Bennett CL, van Rijn E, Jung S, Inaba K, Steinman RM, Kapsenberg ML, Clausen BE. Inducible ablation of mouse Langerhans cells diminishes but fails to abrogate contact hypersensitivity. J Cell Biol. 2005; 169:569–576. [PubMed: 15897263]
14. Kissenpfennig A, Henri S, Dubois B, Laplace-Builhé C, Perrin P, Romani N, Tripp CH, Douillard P, Leserman L, Kaiserlian D, Saeland S, Davoust J, Malissen B. Dynamics and function of Langerhans cells in vivo: dermal dendritic cells colonize lymph node areas distinct from slower migrating Langerhans cells. Immunity. 2005; 22:643–654. [PubMed: 15894281]
15. Swiecki M, Gilfillan S, Vermi W, Wang Y, Colonna M. Plasmacytoid dendritic cell ablation impacts early interferon responses and antiviral NK and CD8(+) T cell accrual. Immunity. 2010; 33:955–966. [PubMed: 21130004]
16. Takagi H, Fukaya T, Eizumi K, Sato Y, Sato K, Shibazaki A, Otsuka H, Hijikata A, Watanabe T, Ohara O, Kaisho T, Malissen B, Sato K. Plasmacytoid Dendritic Cells Are Crucial for the Initiation of Inflammation and T Cell Immunity In Vivo. Immunity. 2011; 35:958–971. [PubMed: 22177923]
17. Fukaya T, Murakami R, Takagi H, Sato K, Sato Y, Otsuka H, Ohno M, Hijikata A, Ohara O, Hikida M, Malissen B, Sato K. Conditional ablation of CD205+ conventional dendritic cells impacts the regulation of T-cell immunity and homeostasis in vivo. Proceedings of the National Academy of Sciences of the United States of America. 2012; 109:11288–11293. [PubMed: 22736794]
18. Piva L, Tetlak P, Claser C, Karjalainen K, Renia L, Ruedl C. Cutting Edge: Clec9A+ Dendritic Cells Mediate the Development of Experimental Cerebral Malaria. The Journal of Immunology. 2012
19. van Blijswijk J, Schraml BU, Reis e Sousa C. Advantages and limitations of mouse models to deplete dendritic cells. European journal of immunology. 2013; 43:22–26. [PubMed: 23322690]

20. Tittel AP, Heuser C, Ohliger C, Llanto C, Yona S, Hämmerling GJ, Engel DR, Garbi N, Kurts C. Functionally relevant neutrophilia in CD11c diphtheria toxin receptor transgenic mice. Nat Methods. 2012; 9:385–390. [PubMed: 22367054]
21. Jiao J, Dragomir A-C, Kocabayoglu P, Rahman AH, Chow A, Hashimoto D, Leboeuf M, Kraus T, Moran T, Carrasco-Avino G, Friedman SL, Merad M, Aloman C. Central Role of Conventional Dendritic Cells in Regulation of Bone Marrow Release and Survival of Neutrophils. The Journal of Immunology. 2014
22. Friedrich G, Soriano P. Promoter traps in embryonic stem cells: a genetic screen to identify and mutate developmental genes in mice. Genes Dev. 1991; 5:1513–1523. [PubMed: 1653172]
23. Buch T, Heppner FL, Tertilt C, Heinen TJAJ, Kremer M, Wunderlich FT, Jung S, Waisman A. A Cre-inducible diphtheria toxin receptor mediates cell lineage ablation after toxin administration. Nat Methods. 2005; 2:419–426. [PubMed: 15908920]
24. Caton ML, Smith-Raska MR, Reizis B. Notch-RBP-J signaling controls the homeostasis of CD8- dendritic cells in the spleen. J Exp Med. 2007; 204:1653–1664. [PubMed: 17591855]
25. Rickert RC, Roes J, Rajewsky K. B lymphocyte-specific, Cre-mediated mutagenesis in mice. Nucleic Acids Res. 1997; 25:1317–1318. [PubMed: 9092650]
26. Lahl K, Loddenkemper C, Drouin C, Freyer J, Arnason J, Eberl G, Hamann A, Wagner H, Huehn J, Sparwasser T. Selective depletion of Foxp3+ regulatory T cells induces a scurfy-like disease. J Exp Med. 2007; 204:57–63. [PubMed: 17200412]
27. Sun C-M, Hall JA, Blank RB, Bouladoux N, Oukka M, Mora JR, Belkaid Y. Small intestine lamina propria dendritic cells promote de novo generation of Foxp3 T reg cells via retinoic acid. J Exp Med. 2007; 204:1775–1785. [PubMed: 17620362]
28. Moussion C, Girard J-P. Dendritic cells control lymphocyte entry to lymph nodes through high endothelial venules. Nature. 2011; 479:542–546. [PubMed: 22080953]
29. Wendland M, Willenzon S, Kocks J, Davalos-Misslitz AC, Hammerschmidt SI, Schumann K, Kremmer E, Sixt M, Hoffmeyer A, Pabst O, Förster R. Lymph node T cell homeostasis relies on steady state homing of dendritic cells. Immunity. 2011; 35:945–957. [PubMed: 22195748]
30. van de Pavert SA, Ferreira M, Domingues RG, Ribeiro H, Molenaar R, Moreira-Santos L, Almeida FF, Ibiza S, Barbosa I, Goverse G, Labão-Almeida C, Godinho-Silva C, Konijn T, Schooneman D, O'Toole T, Mizee MR, Habani Y, Haak E, Santori FR, Littman DR, Schulte-Merker S, Dzierzak E, Simas JP, Mebius RE, Veiga-Fernandes H. Maternal retinoids control type 3 innate lymphoid cells and set the offspring immunity. Nature. 2014; 508:123–127. [PubMed: 24670648]

Europe PMC Funders Author Manuscripts

Europe PMC Funders Author Manuscripts

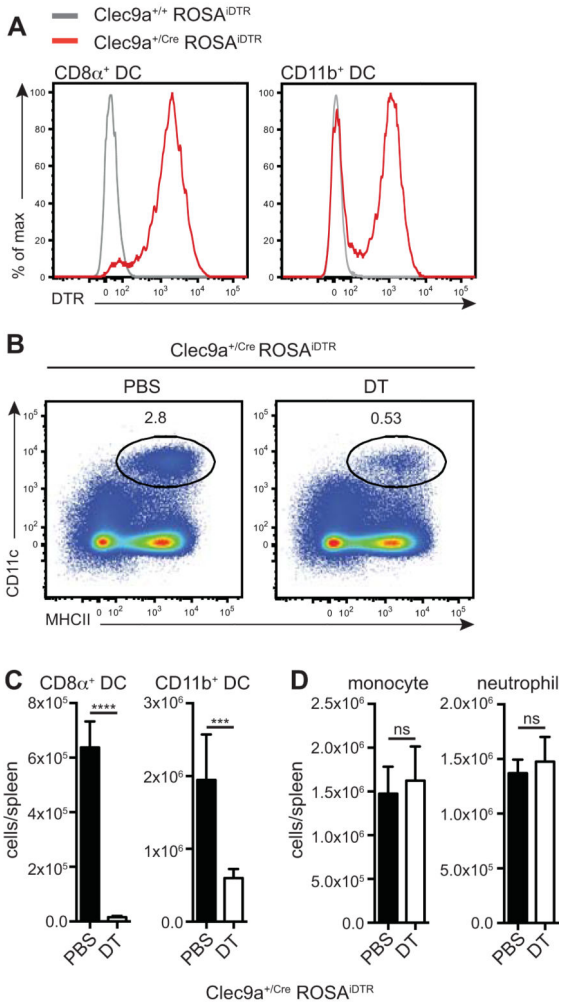

Figure 1. Efficient DC depletion in spleens of DT-injected Clec9a$^{+/cre}$ROSA^{iDTR} mice

(A) CD8α$^+$ DCs (CD11c$^+$ MHCII$^+$ CD8α$^+$) and CD11b$^+$ DCs (CD11c$^+$ MHCII$^+$ CD11b$^+$) in spleen were stained with a polyclonal anti-DTR antibody and analyzed by flow cytometry. Each plot is representative of at least 6 mice per group. (B-D) Mice were injected with DT or PBS and sacrificed 24h later. (B-D) CD8α$^+$ DCs (CD11c$^+$ MHCII$^+$ CD8α$^+$) and CD11b$^+$ DCs (CD11c$^+$ MHCII$^+$ CD11b$^+$) in spleen were identified by flow cytometry. (B) Representative plots of spleen for PBS and DT treated Clec9a$^{+/Cre}$ROSA^{iDTR} mice (gated on live, autofluorescence$^-$ cells). Frequency of gated population is shown. (C) Total CD8α$^+$ DCs and CD11b$^+$ DCs in spleen of PBS- and DT-treated Clec9a$^{+/Cre}$ROSA^{iDTR} mice. (D) The total counts of monocytes (CD11b$^+$ Ly6c$^+$ Ly6g$^-$) and neutrophils (CD11b$^+$ Ly6g$^+$) per spleen of PBS and DT treated Clec9a$^{+/Cre}$ROSA^{iDTR} mice is shown. Ns: non significant, ***: p≤0.001, ****: p≤0.0001. This experiment was performed twice with 4-7 mice per group. One representative experiment is shown.

Europe PMC Funders Author Manuscripts

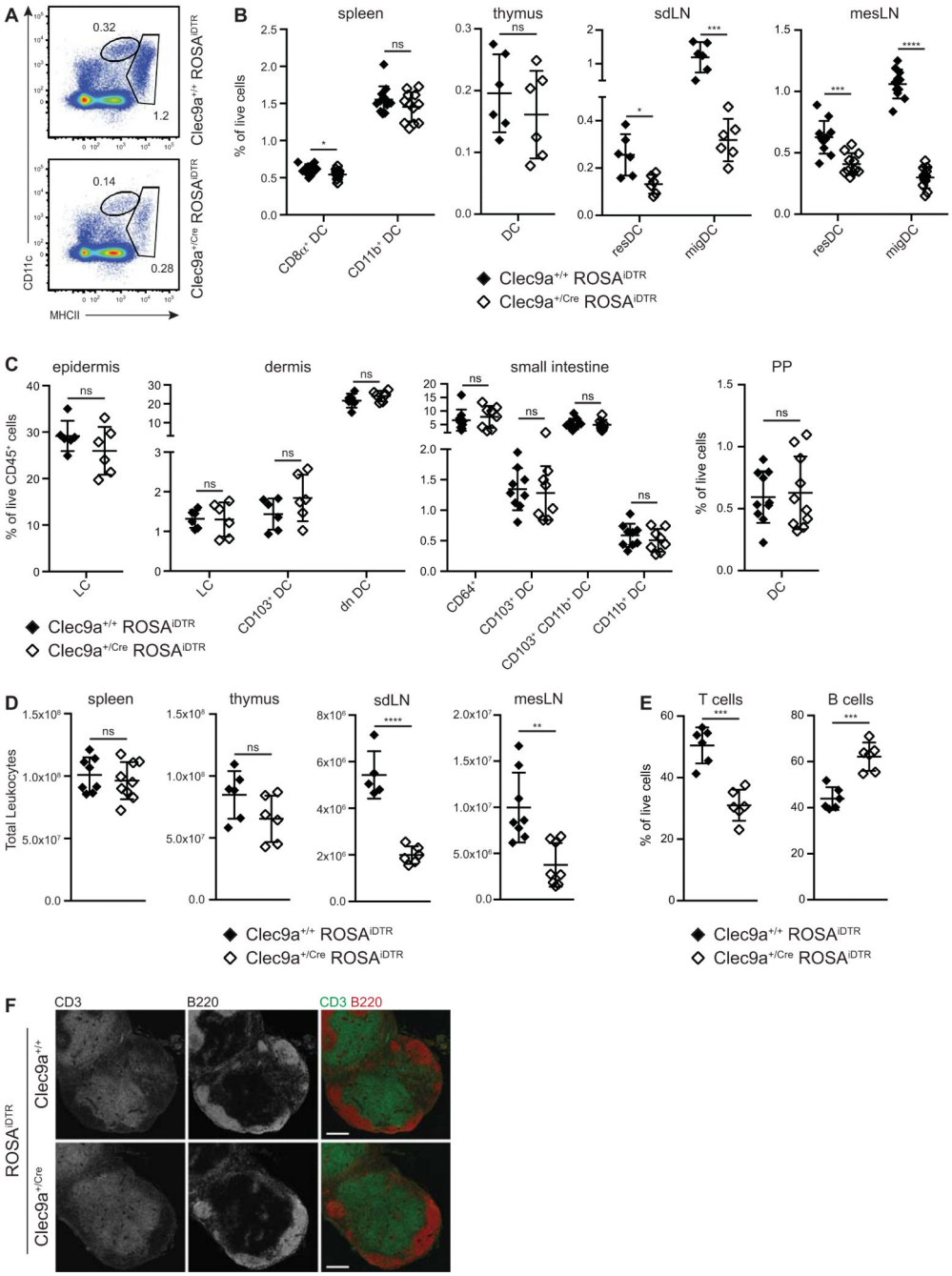

Figure 2. LNs, but not spleen, thymus or non-lymphoid tissues of Clec9a$^{+/Cre}$ROSA^{iDTR} mice display hypocellularity and reduced DC frequency

(A) Representative plots of sdLNs of control and Clec9a$^{+/Cre}$ROSA^{iDTR} mice, gated on live cells. (B) CD8α^{+} DCs (CD11c^{+} MHCII^{+} CD8α^{+}) and CD11b^{+} DCs (CD11c^{+} MHCII^{+} CD11b^{+}) in spleen, DCs in thymus (CD11c^{+} MHCII^{+}) and resDCs (CD11c^{+} MHCII^{int}) and migDCs (CD11c^{+} MHCII^{hi}) in sdLNs and mesLNs of control and Clec9a$^{+/Cre}$ROSA^{iDTR} mice were identified by flow cytometry and DC subsets as percentage of live leukocytes are plotted. (C) The frequency of Langerhans cells (LCs, MHCII^{+} CD64^{-} EpCAM^{hi}), CD103^{+} DCs (MHCII^{+} CD64^{-} CD103^{+}) and double negative DCs (dn DCs, MHCII^{+} CD64^{-}

CD103^{-} EpCAM^{-}) in epidermis and dermis of control and Clec9a$^{+/Cre}$ROSA^{iDTR} mice is shown (left two panels). The frequency of CD64^{+} cells (CD11c^{+} MHCII^{+} CD64^{+}), CD103^{+} DCs (CD11c^{+} MHCII^{+} CD64^{-} CD103^{+} CD11b^{-}), CD103^{+} CD11b^{+} DCs (CD11c^{+} MHCII^{+} CD64^{-} CD103^{+} CD11b^{+}) and CD11b^{+} DCs (CD11c^{+} MHCII^{+} CD64^{-} CD103^{-} CD11b^{+}) in the small intestine and DCs (CD11c^{+} MHCII^{+}) in the Peyer's Patches (PP) of control and Clec9a$^{+/Cre}$ROSA^{iDTR} mice is shown (right two panels). (D) Single-cell suspensions of spleen, thymus, sdLNs and mesLNs from control and Clec9a$^{+/Cre}$ROSA^{iDTR} mice were counted and the number of total leukocytes is plotted. (E) T cells (CD3^{+} MHCII^{-}) and B cells (MHCII^{+} CD11c^{-}) in mesLNs of control and Clec9a$^{+/Cre}$ROSA^{iDTR} mice were identified by flow cytometry and T cells and B cells as percentage of live leukocytes are plotted. (B-E) Each dot represents one mouse. Ns: non significant, *: $p \leq 0.05$, **: $p \leq 0.01$, ***: $p \leq 0.001$, ****: $p \leq 0.0001$. Data are pooled from at least two independent experiments. (F) Frozen sections of sdLNs from control and Clec9a$^{+/cre}$ROSA^{iDTR} mice were stained with anti-CD3 and anti-B220 antibodies and imaged by confocal microscopy. Scale bar: 300μm. Images are representative of 3 mice per group.

Europe PMC Funders Author Manuscripts

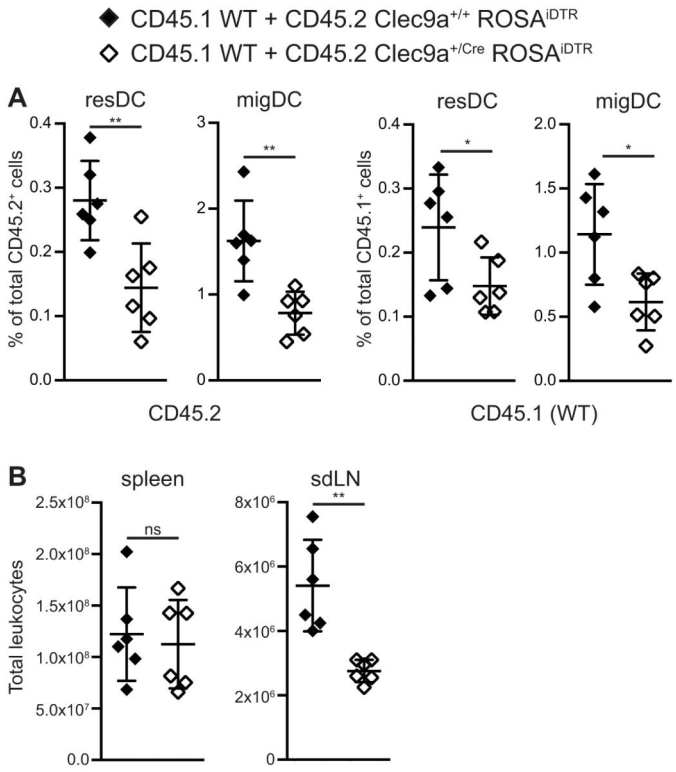

Figure 3. In mixed bone marrow chimeras the phenotype conferred by Clec9a$^{+/Cre}$ROSA^{iDTR} bone marrow is dominant

CD45.2^{+} C57BL/6J hosts were lethally irradiated and reconstituted with a 1:1 mixture of CD45.1^{+} WT and CD45.2^{+} Clec9a$^{+/+}$ROSA^{iDTR} or Clec9a$^{+/Cre}$ROSA^{iDTR} BM. Mice were analyzed 7 months after BM transfer.

(A) Single cell suspensions of sdLNs were analyzed by flow cytometry. CD45.1^{+} and CD45.2^{+} cells were identified and within these fractions resDCs (CD11c^{+} MHCII^{int}) and migDCs (CD11c^{+} MHCII^{hi}) were gated. Frequencies of resDCs and migDCs within the CD45.2^{+} or CD45.1^{+} fraction are plotted. (B) Total leukocyte numbers of spleens and sdLNs are plotted. Each dot represents one mouse. Ns: non significant, *: p≤0.05, **: p≤0.01. Data are representative of two independent experiments.

Europe PMC Funders Author Manuscripts

Europe PMC Funders Author Manuscripts

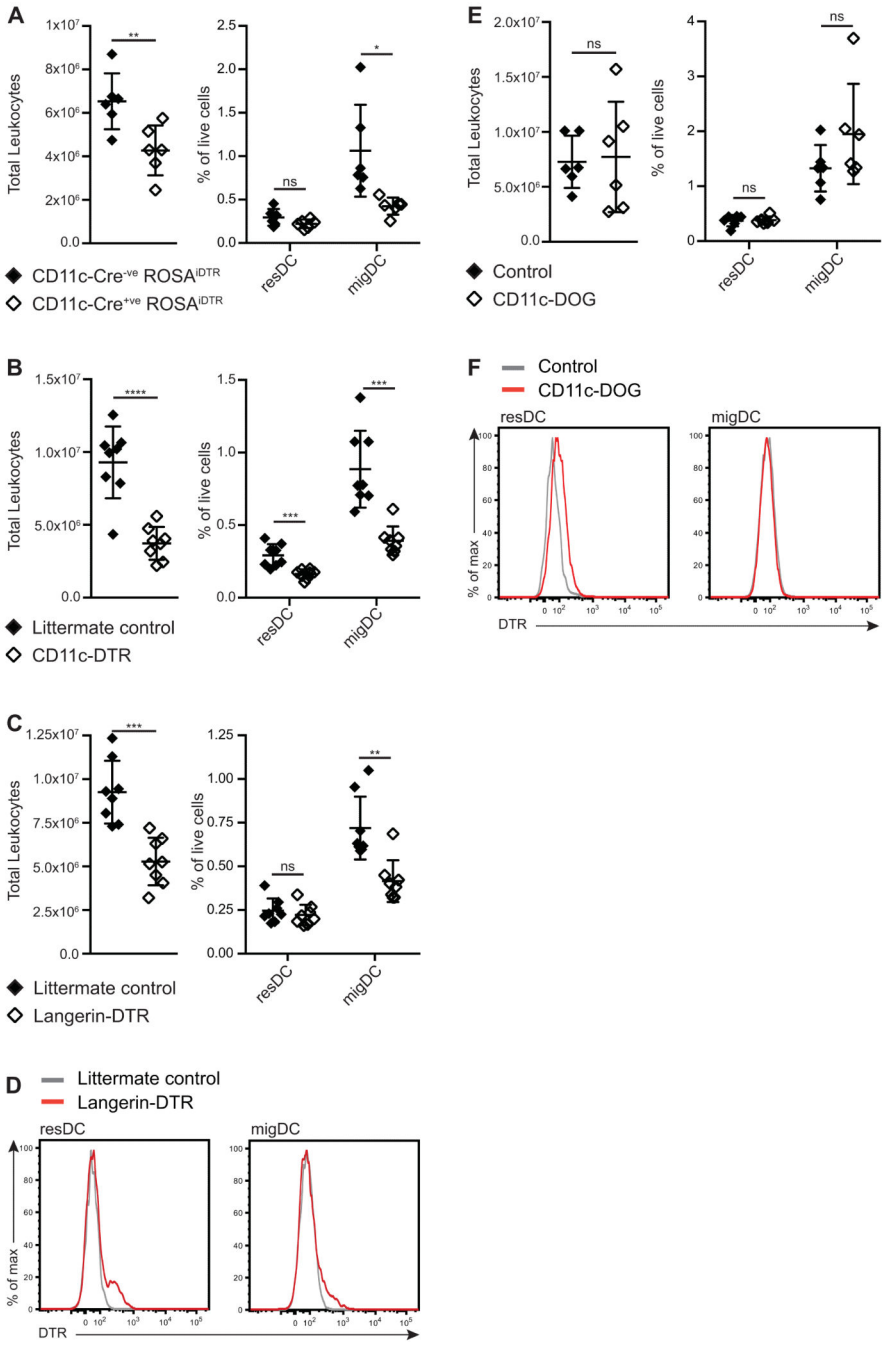

Figure 4. Other mouse models in which DTR is expressed on migDCs display hypocellularity and reduced DC frequency in sdLNs

(A-C) SdLNs of CD11c-Cre^{+ve}ROSA^{iDTR} (A) CD11c-DTR (B) and Langerin-DTR (C) mice were analyzed for total cellularity (left panel) and frequency of resDCs (CD11c^{+} MHCII^{int}) and migDCs (CD11c^{+} MHCII^{hi}) (right panel). (D) ResDCs (CD11c^{+} MHCII^{int}) and migDCs (CD11c^{+} MHCII^{hi}) in sdLNs from Langerin-DTR mice were stained with a polyclonal anti-DTR antibody and analyzed by flow cytometry. (E) SdLNs from CD11c-DOG mice were analyzed as in A-C. (F) DTR expression on resDCs and migDCs in sdLNs from CD11c-DOG mice was analyzed as in D. (A-C,E) Each dot represents one mouse. Data

are pooled from at least two independent experiments. Ns: non significant, *: p≤0.05, **: p≤0.01 ***: p≤0.001, ****: p≤0.0001. (B,F) Each plot is representative of 6-8 mice per group.

Europe PMC Funders Author Manuscripts

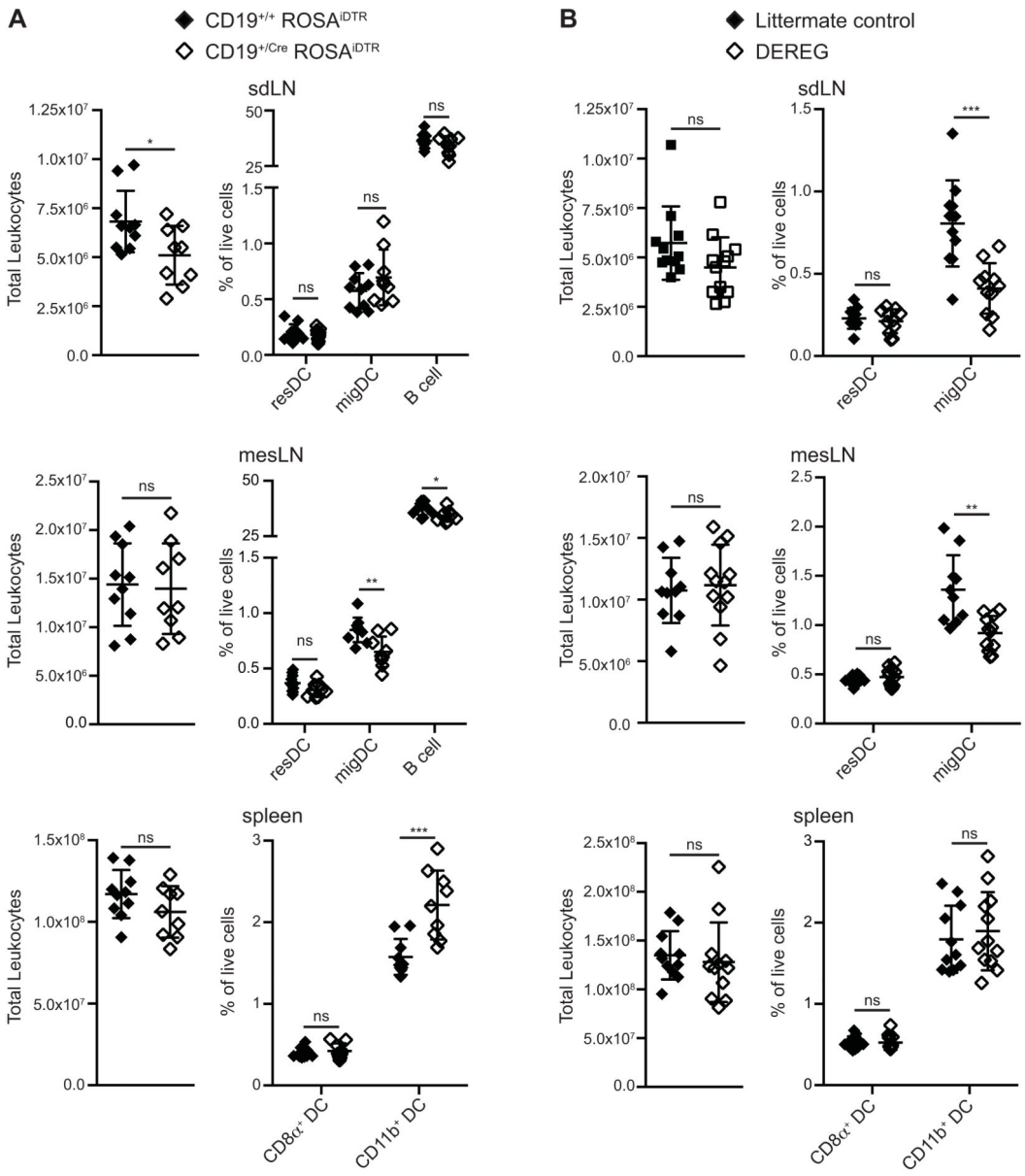

Figure 5. Expression of DTR on B cells or Tregs does not lead to overall LN hypocellularity and reduced frequencies of LN DCs

Left panels: single-cell suspensions of sdLNs, mesLNs and spleen from control and $CD19^{+/Cre}ROSA^{iDTR}$ mice (A) or DEREG mice (B) were counted and the number of total leukocytes is plotted. Right panels: resDCs ($CD11c^{+}$ $MHCII^{int}$) and migDCs ($CD11c^{+}$ $MHCII^{hi}$) in sdLNs and mesLNs and $CD8\alpha^{+}$ DCs ($CD11c^{+}$ $MHCII^{+}$ $CD8\alpha^{+}$), $CD11b^{+}$ DCs ($CD11c^{+}$ $MHCII^{+}$ $CD11b^{+}$) and B cells ($CD11c^{-}$ $MHCII^{+}$, $CD19^{+/Cre}ROSA^{iDTR}$ mice only) in spleen of control and $CD19^{+/Cre}ROSA^{iDTR}$ mice (A) or DEREG mice (B) were identified by flow cytometry and DC subsets as percentage of live leukocytes are plotted. Each dot represents one mouse. Data are pooled from at least two independent experiments. Ns: non significant, *: $p \leq 0.05$, **: $p \leq 0.01$ ***: $p \leq 0.001$.

Europe PMC Funders Author Manuscripts